

Research paper

# Physicochemical and cell adhesion properties of chitosan films prepared from sugar and phosphate-containing solutions

Ruggero Bettini <sup>a,\*</sup>, Antonello A. Romani <sup>b</sup>, Marina M. Morganti <sup>b</sup>, Angelo F. Borghetti <sup>b</sup>

<sup>a</sup> Department of Pharmacy, University of Parma, Italy

<sup>b</sup> Department of Experimental Medicine – Section of Molecular Pathology and Immunology, University of Parma, Italy

Received 4 December 2006; accepted in revised form 22 March 2007

Available online 18 July 2007

## Abstract

This work was aimed at investigating a series of chitosan films obtained from chitosan, chitosan-phosphate, chitosan-phosphate-D-(+)raffinose or chitosan-phosphate-D-(+)sucrose solutions to preliminarily select a suitable biomaterial for developing a cell substrate for tissue engineering. The prepared films were characterized in terms of physicochemical properties (FT-IR, XRD, optical microscopy, wettability, water absorption, and tensile stress) and effects on proliferation of different types of human cells (endothelial, HUVEC; fibroblast, WI-38).

The obtained results indicated that the presence of sucrose or raffinose at high concentration along with phosphate salts in the chitosan film-forming solution affords smooth, amorphous and highly hydrophilic materials in the form of soft and elastic film with optimal cytocompatibility.

Owing to improved physicochemical and mechanical properties as well as affinity for differentiated human cells, these novel chitosan films appear as promising candidate biomaterials for tissue regeneration and repair.

The major finding is the possibility to improve the biocompatibility of chitosan films by simply modifying their solid state characteristics.

© 2007 Elsevier B.V. All rights reserved.

**Keywords:** Chitosan film; Sugars; Swelling index; Surface characterization; Mechanical properties; Human cell culture; Cytocompatibility; Cell proliferation

## 1. Introduction

Tissue and organ failure accounts for a large portion of healthcare expenditure worldwide [1,2]. Injury and disease can affect tissues such as skin or bone marrow or more complex organs like kidneys, liver, or heart. Treatment options for these diseases and injuries include drug therapy, surgical repair, prosthetic device and mechanical support and transplants; however, these treatments often provide unsatisfactory repair or maintenance. Prosthetic and mechanical support devices do not replace the full

and proper function of the damaged tissue or organ, which often leads to continued disease progression or possible systemic infection. In the case of transplantation, donor shortage [3] and problems related with immuno-suppression are major issues still to be addressed. Because these options do not always provide satisfactory restoration of organ and/or tissue function, other avenues to restore, repair, and/or maintain tissues and organs are pursued. One of these avenues is represented by the emerging science of tissue engineering which involves the use of components, either synthetic or natural, to create or replace parts of damaged/diseased tissues and organs [1,4]. This approach may be achieved by the following three sequential steps: (i) developing a substrate that should be biocompatible, biodegradable, sterilizable, and with a optimal surface on which new tissue can grow, (ii) creating models to study

\* Corresponding author. Department of Pharmacy, Viale G.P. Usberti 27/A, University of Parma, 43100 Parma, Italy. Tel.: +39 0 521905089; fax: +39 0 521905006.

E-mail address: [bettini@unipr.it](mailto:bettini@unipr.it) (R. Bettini).

three-dimensional tissue organization, (iii) providing replacement parts or cellular prostheses for the human body. Then in parallel tissue engineering can also provide suitable vehicles to deliver drug or engineered cells to disease-affected tissues/organs.

Over the last years chitosan has received increased attention as one of the promising polymeric materials with a large number of applications in the pharmaceutical and biomedical industries.

Chitosan is a cationic natural biopolymer produced by alkaline N-deacetylation of chitin, the most abundant natural polymer after cellulose [5]. It becomes an interesting biomaterial due to its good biocompatibility, biodegradability, low toxicity and low cost [6]. It has been extensively used over a wide range of applications, such as drug carriers, chelating agents, membrane filter for water treatment, and biodegradable [7–10] coating or film for food packaging [11–15]. Recently, the potential value of chitosan and its derivatives in wound healing, tissue-engineering and gene therapy has been investigated [16].

In the present work we investigated a series of chitosan films prepared from chitosan, chitosan-phosphate, chitosan-phosphate-D-(+)-raffinose or chitosan-phosphate-D-(+)-sucrose solutions. The obtained films were characterized in terms of physicochemical properties (FT-IR, XRD, optical microscopy, wettability, water absorption, and tensile stress) and effects on growth of different types of human cells. The final goal was to preliminarily select a suitable biomaterial for developing a cell substrate for tissue engineering.

## 2. Experimental

### 2.1. Materials

Chitosan powder (deacetylation degree = min 90%, particle size = 60–80 mesh) was purchased from A.C.E.F (Fiorenzuola, Italy). Foetal calf serum (FCS), antibiotics, media D-MEM and MEM for cell culture were purchased from GIBCO (Grand Island, NY, USA). Disposable plastics for laboratory use were obtained from COSTAR (Cambridge, MA, USA). Reagents of analytical grade were obtained from Sigma Chemical Co. (St. Louis, MO, USA).

### 2.2. Methods

#### 2.2.1. Chitosan purification

Four grams of chitosan was dissolved in 200 ml of aqueous acetic acid (1% w/v) with 0.9% (w/v) of NaCl and stirred until complete dissolution of the powder. The chitosan solution was then filtered (0.8  $\mu$ m) under vacuum to remove the insoluble particles. Aqueous KOH solution (3%, w/v) (100 ml) was dropped (50  $\mu$ l/drop) under intensive stirring into the chitosan solution using a peristaltic pump (30 drops/min). The pH of the solution was adjusted between 8 and 9 by adding 1% v/v aqueous acetic acid. After 3 h the cheese-flakes like dispersion of chitosan was

separated from solution by filtration and carefully washed with distilled water until neutrality. Then, it was dehydrated in 400 ml of ethanol (EtOH) under stirring for 2 h, separated by filtration, re-dispersed in 200 ml of EtOH and stirred again for other 2 h. Finally the chitosan dispersion was separated by centrifugation, poured on a Teflon plate and dried at 37 °C for 24 h in a ventilated oven. The final product was ground to powder with pestle and mortar. This process yielded approximately 85% of the initial chitosan weight.

#### 2.2.2. Preparation of chitosan films

Four grams of the purified chitosan powder, obtained with the method above described, was dissolved in a 1% (w/v) acetic acid aqueous solution until complete dissolution. Dibasic sodium phosphate (7.5 mM), sodium dihydrogen phosphate (22 mM), potassium dihydrogen phosphate (1.5 mM), sodium chloride (125 mM) and potassium chloride (2 mM) were then sequentially added. The solution was filtered under vacuum using a 0.8  $\mu$ m filter. Finally, D-(+)-raffinose pentahydrate (in amount ranging from 0.29 to 290 mM) or D-(+)-sucrose (290 mM) was added to the solution and allowed to dissolve for 2 h under gentle stirring. One milliliter of each of the above-mentioned solutions was poured onto microscope slide (12  $\times$  25 mm) to obtain a uniform thickness and dried overnight at 45 °C in a ventilated oven. The film deacetylation was carried out by soaking it into a 3% aqueous KOH for 12 h at room temperature. Finally the films were washed with distilled water until neutrality and stored in distilled water until use. Six different films were prepared and coded as follows: *CH* (from the solution containing only chitosan); *CHP* (from the solution containing chitosan and phosphate salts); *CHPR1*, *CHPR2*, *CHPR3* (from the solution containing chitosan, phosphate salts and D-(+)-raffinose in the amount of 2.9 mM, 29 mM and 290 mM, respectively) and *CHPS* (from the solution containing chitosan, phosphate salts and D-(+)-sucrose).

#### 2.2.3. Microscopy

Images of the fully hydrated films were taken at the 100 $\times$  magnification using an optical microscope image analysis system (Nikon Digital Net System, Japan).

#### 2.2.4. Fourier transform infrared (FT-IR) spectroscopy

Infrared spectra of D-(+)-raffinose, D-(+)-sucrose, chitosan powder or chitosan films were recorded in the 4000–400  $\text{cm}^{-1}$  wavenumber range at ambient temperature at the resolution of 4  $\text{cm}^{-1}$  and 24-times by direct scanning under the objective of the microscope of a microFT-IR spectrophotometer (MFT 2000, Jasco, Japan).

#### 2.2.5. X-ray diffraction (XDS)

X-ray diffraction patterns of the films were measured with a Miniflex diffractometer (Rigaku, Japan) using Cu  $K_{\alpha}$  radiation ( $\lambda = 1.5418 \text{ \AA}$ ) generated with 30 kV and 20 mA. Specimens were prepared by piling 5 films in Al

holders and scanned at room temperature over the  $2\theta$  range  $5\text{--}35^\circ$  with a step size of  $0.5^\circ/\text{min}$ .

#### 2.2.6. Wettability

Contact angle measurements were performed at room temperature with a goniometer (AB Lorentzen & Wettre, Germany). A drop of double distilled water ( $4\ \mu\text{L}$ ) was placed on the surface of the dry film. Images of the water droplet were recorded within 10 s of deposition by means of a digital camera (FinPix S602 Zoom, Fuji film, Japan). Digital pictures were analyzed by ImageJ 1.28v software (NIH, USA) for angle determination. A minimum of five measurements, taken at different positions on the film, was carried out. The contact angles were measured on both sides of the drop and averaged.

#### 2.2.7. Swelling index

The swelling index,  $S_w$ , of the prepared films was determined according to the following equation:

$$S_w = \frac{W_s - W_d}{W_d} \quad (1)$$

where  $W_s$  and  $W_d$  represent the weights of the fully hydrated and the dry film, respectively.

#### 2.2.8. Mechanical properties

The film thickness was measured with a thickness tester (Mitutoyo, Japan, accuracy  $0.001\ \text{mm}$ ). Five values were randomly taken at different locations for each specimen used in the tensile tests.

Films in the fully hydrated state were mechanically tested in stretching mode at constant rate ( $15\ \text{mm/min}$ ) until break by means of a tensile tester (AG MC1, Acquat, Italy). Force and time signal were digitalized by means of a PowerLab 400 board and recoded with a Scope 3.5 software running on a Macintosh Powerbook G3 computer. Young's modulus and elongation at break for each film were calculated from the relevant stress–strain curves.

#### 2.2.9. Cell culture

All studies were performed using human diploid fibroblasts (HDF, cell strain WI-38) derived from female foetal lung, and human endothelial cells derived from foetal umbilical vessels (HUVEC). Cells were provided by the American Type Culture Collection (Rockville, MD, USA) and obtained through the Istituto Zooprofilattico Sperimentale (Brescia, Italy). Cultures were maintained in complete medium (D-MEM containing antibiotics and 10% foetal calf serum). HUVEC cells were cultured in complete medium supplemented with  $50\ \mu\text{g ml}^{-1}$  of endothelial cell growth factor. All cultures were kept in a incubator at  $37^\circ\text{C}$  in a water-saturated atmosphere with 5%  $\text{CO}_2$ .

Routine sub-cultivations were carried out every week. When cells reached confluence they were harvested by treatment with 0.25% trypsin in phosphate-buffered saline (PBS) at pH 7.5, counted in a Bürker haemocytometer and plated at a density of  $1 \times 10^4\ \text{cells cm}^{-2}$  [17].

#### 2.2.10. Cell proliferation

Fibroblasts were seeded onto chitosan films as well as on tissue culture polystyrene (TCPS, Corning, USA) at a density of  $1\text{--}2.5 \times 10^4\ \text{cells cm}^{-2}$  in a 24-well plate. The cells were maintained in complete medium that was refreshed every 3 days. Assay was performed on different plate at 1, 4 and 7 days, respectively. At each time interval, the monolayers were rinsed twice with PBS solution and then the cells were detached from the substrate by 0.25% trypsin in PBS. The number of adherent cells was counted with a Bürker haemocytometer.

#### 2.2.11. Cell morphology

For morphological characterization, fibroblasts cultured on chitosan films were examined by contrast-phase and scanning electron microscopy (SEM). After being cultured for 7 days, the cell monolayer adherent to the film was gently washed with PBS three times. Then the film was fixed with 2.5% glutaraldehyde in PBS for 1 h at  $4^\circ\text{C}$ . After thorough washing with PBS, the cells were dehydrated through critical point drying. The films were mounted on glass slides with double-sided adhesive tape, then gold sputter coated under vacuum to a thickness of  $100\text{--}200\ \text{\AA}$  and examined using a Cambridge StereoScan 2000 microscope at 10 kV.

#### 2.2.12. Statistical analysis

Data were expressed as means  $\pm$  standard deviation (SD). Measurements were conducted at least in triplicate. Student's *t*-test on unpaired data was used to assess the statistical significance of the difference between the physico-chemical parameters measured on different films (Kaleida-Graph®, Synergy Software, USA). Statistical significance was assumed at a confidence level of 95% ( $p < 0.05$ ).

### 3. Results and discussion

#### 3.1. Physico-chemical characterization

The FT-IR spectra analysis of the chitosan films was based on the identification of the absorption bands relevant to vibration of functional groups of chitosan. The band wavenumbers were assigned according to Pawlak and Mucha [18]. In general the incorporation of phosphate salts and D-(+)-raffinose or D-(+)-sucrose in the chitosan solution used for film preparation led to nondramatic modifications in the IR spectrum of chitosan. Table 1 reports the wavenumbers of the band in the  $1700\text{--}1500\ \text{cm}^{-1}$  region: the amide I band ( $\text{C=O}$  in amide group) wavenumber was lower than the value for chitosan powder ( $1664\ \text{cm}^{-1}$ ) for all the prepared films and particularly for the CH film ( $1649\ \text{cm}^{-1}$ ) and CHPR1 ( $1647\ \text{cm}^{-1}$ ). This might be interpreted as the result of a lower mobility of the  $\text{C=O}$  group in the films due to its involvement in the formation of a weak bound in the solid structure. The incorporation of phosphate salts and significant amount of sugars in the chitosan solution used for film preparation seems to reduce this effect. On

Table 1

Absorption bands ( $\text{cm}^{-1}$ ) associated with vibration of characteristic functional groups in chitosan powder and dry chitosan films prepared from different solutions

Functional group	Chitosan powder	Film					
		CH	CHP	CHPR1	CHPR2	CHPR3	CHPS
C=O in amide group (Amide I band)	1664	1649	1652	1647	1655	1653	1653
NH <sub>2</sub> in amino group	1592	1588	1588	1585	1589	1590	1591
CH <sub>3</sub> in amide group	1379	1377	1378	1375	1378	1377	1377
C–O group	1261	1255	1254	1254	1254	1257	1259

the other hand the amino group band of CH, CHP and CHP2 films was at lower wavenumbers ( $1588\text{ cm}^{-1}$ ) than that of the chitosan powder ( $1592\text{ cm}^{-1}$ ), while it was practically unchanged in the CHPR3 and CHPS films ( $1590$  and  $1591\text{ cm}^{-1}$ , respectively).

D-(+)-Raffinose FT-IR spectrum evidenced characteristics bands at  $2936$  and  $1649\text{ cm}^{-1}$ . While the latter is attributable to the scissoring vibration mode of the crystal water in the D-(+)-raffinose pentahydrate, the first band is substantially independent of dehydration [19]. Interestingly, no trace of this last band was found in the FT-IR spectra of the chitosan films prepared from solutions containing an amount of D-(+)-raffinose ranging from  $2.9$  to  $290\text{ mM}$ . Similarly, no trace of the characteristic series of peaks between  $2994$  and  $2914\text{ cm}^{-1}$  of the sucrose powder [20] was found in the CHPS film spectrum.

These observations may allow speculating that the excipients added to chitosan in the film forming solutions are not recovered in the solid film but they interacted or interfered with chitosan chains during the film formation process giving rise to final products slightly differing from each other in the structure of the solid state.

Fig. 1 illustrates the appearance of fully hydrated CH, CHP, CHPR3 and CHPS films as seen through an optical microscope at  $100\times$  magnification. A clear difference in the surface structure can be observed: the CH film (panel a) presented a micropatterned topography which was dramatically magnified in the CHP film (panel b) where tree-like morphology can be clearly observed. Interestingly a similar organization was reported by Cai et al. for gelatin layer in titanium–chitosan–gelatin multilayer film [21]. This kind of structure was observed in the CHPR1 and CHPR2 films as well. On the contrary, the film obtained from the D-(+)-raffinose ( $290\text{ mM}$ ) or D-(+)-sucrose solution (panels c and d) showed a uniform and smooth surface suggesting absence of an organization detectable at a microscopic level.

In spite of the great differences in the film's appearance, X-ray diffraction patterns obtained from the different films were only slightly different from each other, all being characterized by a unique broad peak indicating an amorphous structure. In particular CH, CHP, CHPR1 and CHPR2 presented a more defined diffraction peak, while CHPR3 and CHPS were characterized by a smoother diffraction pattern. This would allow us to hypothesize that the structural differences observed between the hydrated films are somewhat maintained in the dry state. However, it should be stated that the resolution capability of the used diffrac-

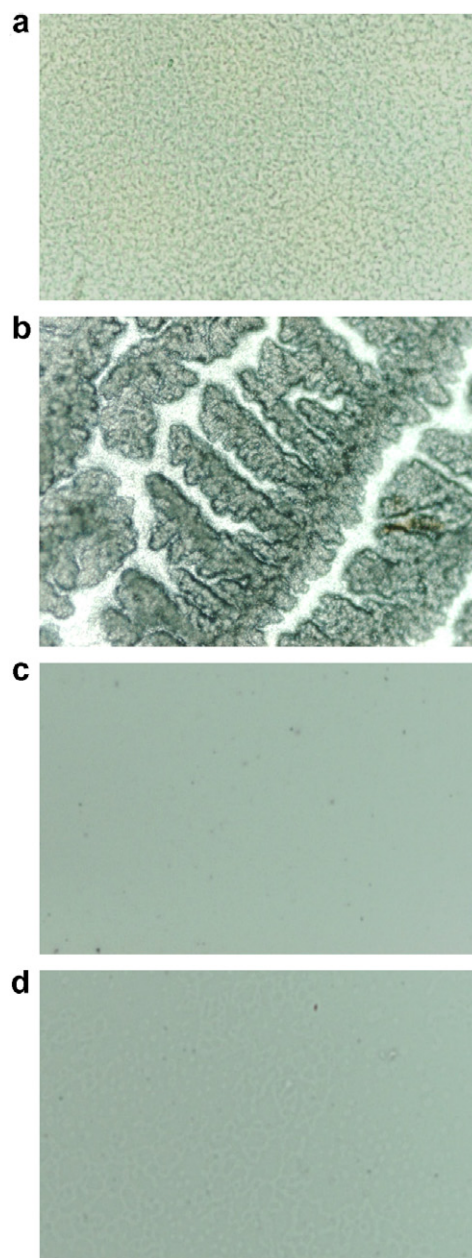


Fig. 1. Pictures taken at the optical microscope ( $100\times$ ) of fully hydrated CH (a); CHP (b); CHPS (c) and CHPR3 (d) films.

tometer might not be enough to evidence differences in the degree of crystallinity of polymeric films.

As far as the surface characteristics are concerned, wettability has been shown to be an important attribute for



cell attachment to chitosan substrate [22,23]. Contact angle measurements were performed on CH, CHPR3 and CHPS films. The relevant water contact angles are reported in Table 2. CH film showed the least wettable surfaces with significantly higher contact angle with respect to CHPS and CHPR3 ( $p < 0.005$ ). CHPR3 was the most hydrophilic material as it presented the lowest contact angle, although the difference with the value of the CHPS film was not highly statistically significant ( $p = 0.07$ ).

Hydrophilicity of the films was also investigated by measuring the swelling index in water at the equilibrium (Table 2). These data confirmed the highest hydrophilicity of the films obtained by adding a sugar to the solution used for the film preparation in comparison to the film obtained from a solution containing only chitosan. In fact, CH film showed quite a high affinity for water, increasing more than 300 times its initial weight. CHPS and CHPR3 films, however, were characterized by a much higher degree of swelling, affording a weight at the equilibrium more than 3 orders of magnitude higher than that of the dry film.

The mechanical properties of the prepared films were studied in stretching until break. The Young's modulus,  $E$ , was calculated from the slope of the linear part of the stress *vs* strain curve according to the equation [24]:

$$\frac{F}{A} = E \left( \frac{L - L_0}{L_0} \right) \quad (2)$$

where  $F$  is the force applied on the cross-sectional area  $A$ ,  $L$  is the obtained elongation and  $L_0$  is the initial length of the film.

All films but CH showed solely an elastic behavior. The CH film presented also a small portion of plastic behavior at the end of the linear part of the stress/strain curve (nearly 5% elongation at almost constant stress). Table 3 summarizes the mechanical properties of the prepared films. It can be observed that all films did not show any sta-

tistically significant difference in elongation at break that resulted in all cases between 30% and 60%. However, the elastic modulus was significantly higher for CHPR3 and CHPS films with respect to CH, CHPR1 and CHPR2 films ( $p < 0.05$ ) indicating a higher mechanical resistance for the films prepared from solutions containing 290 mM of sugar.

### 3.2. Cell adhesion and proliferation

The cell behavior on materials is the key factor for evaluation of the cytocompatibility of a novel biomaterial. Cell adhesion, spreading, proliferation and differentiation are the sequential reactions that follow cell seeding and are crucial steps to estimate optimal cell survival on novel materials.

Several modifications of chitosan surfaces have been reported to improve cell adhesion, increase cell proliferation and improve cell yields [16]. We have evaluated the effects of adding phosphate and sugars to the chitosan film-forming solutions on cell growth of different types of human cells. Only two of the prepared chitosan films (CHPR3 and CHPS) afforded a beneficial effect on three aspects of cell culture: (i) rate of attachment and initiation of cell doubling, (ii) robustness of attachment and

Table 2  
Static contact angle (°) with water and swelling index at the equilibrium (%) in water of different chitosan films

	Film		
	CH	CHPR3	CHPS
Contact angle (°)	59.5 (1.0)	27.4 (2.7)	38.7 (1.7)
Swelling index (%)	343	1285	1097

Standard deviation in parentheses.

Table 3  
Young's modulus and percentage of elongation at break of chitosan films prepared from different solutions

Film	Young's modulus ( $\text{N m}^{-2}$ ) $\times 10^3$	Elongation at break (%)
CH	106 (10)	54.8 (12)
CHP	44 (12)	36.8 (8.3)
CHPR1	60 (20)	56.2 (39.3)
CHPR2	37 (8)	48.6 (6.6)
CHPR3	242 (20)	31.2 (6.9)
CHPS	210 (20)	34.3 (0.5)

Standard deviation in parentheses.

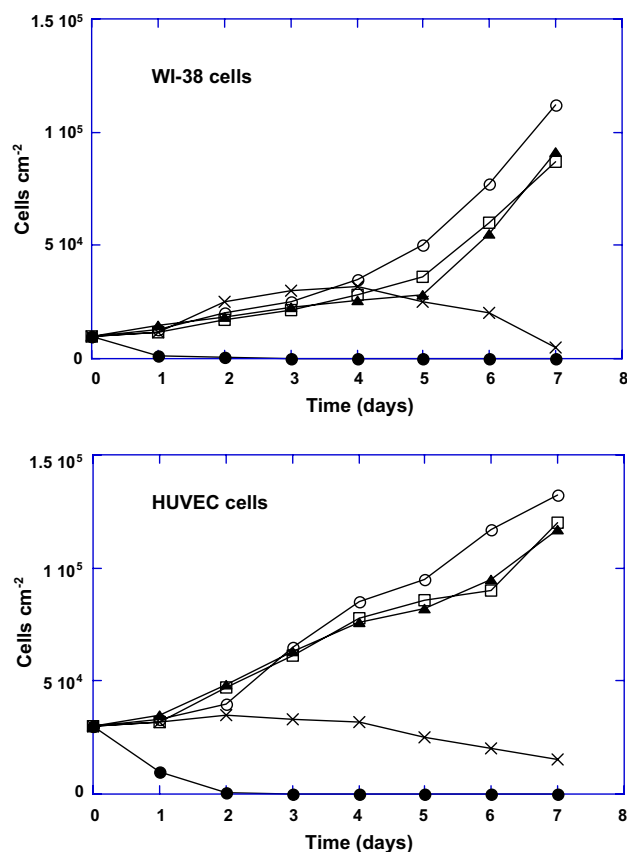


Fig. 2. Number of WI-38 and HUVEC cells per  $\text{cm}^2$  as a function of time after seeding on different films: CH (cross); CHP (solid circle); CHPS (triangle); CHPR3 (square). Control (circle) indicates cells grown on standard plastic culture dishes (TCPS, Corning).

reduction of detachment for cells grown as long as 7 days after seeding, and (iii) the consistency of cells grown on a more uniform surface resulting in higher cell yields.

WI-38 and HUVEC cells were seeded at low density and 24 h later monitored for attachment and spreading to the CH, CHP, CHPR3 and CHPS films in comparison to the surface of standard culture dishes taken as control.

As shown in Fig. 2, WI-38 and HUVEC cells poorly attached and did not grow on CHP film. When both types of cells were cultured on CH film they attached similarly to control. However, after few days cells did not grow, later on a significant portion started to detach from the substratum. In contrast, cell attachment and proliferation rate on CHPR3 and CHPS films were comparable to control cells grown on standard plastic dishes. By using contrast-phase microscopy we did not observe any morphological indication of cell death like apoptosis or anoikis such as slow rounding up of cells, cell shrinkage, surface blebbing, and formation of apoptotic bodies.

Fig. 3 shows the evolution of morphology of both cell types seeded on CHPR3. After 24 h (panel a) WI-38 cells

changed from spherical to flat, meaning that cells after finishing the attachment process were in the spreading phase. At this time, they assumed the spindle morphology of viable human fibroblasts with typical filopodia-like extension; meanwhile most of the HUVEC cells maintained a round shape. Later on, 48 and 72 h after seeding (Fig. 3b and c) WI-38 cells slowly increased their density maintaining the fibroblast-like aspect; in contrast, HUVEC cells changed their morphology from round to a flat, cobblestone-like shape, proliferated and started to aggregate, forming a network of colonies. Interestingly, in some areas the endothelial cells arranged in circular structures that resemble sections of capillaries (see arrowhead in panel C right).

After 7 days of seeding and culturing on CHPR3 and CHPS films as well as on standard culture plastic dishes, HUVEC cell morphology was also analyzed at higher magnification via SEM. The cells formed a homogeneous monolayer exhibiting the typical characteristics (flatness and cobblestone-like appearance) of endothelial cells, with several intercellular junctions clearly visible (Fig. 4). On the contrary, when cultured on CH, CHP, CHPR1 or CHPR2

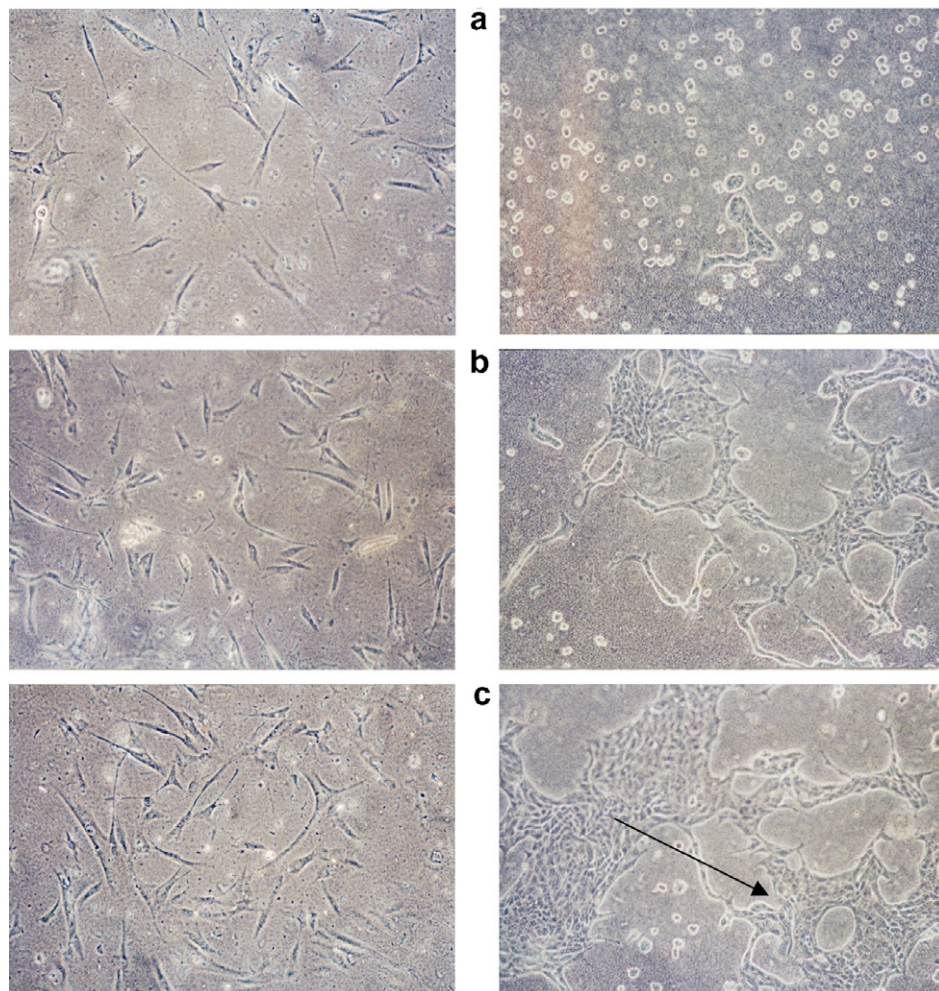


Fig. 3. Pictures taken at the optical microscope in phase contrast (magnification 100 $\times$ ) of WI-38 (left panels) and HUVEC (right panels) cells seeded at low density on CHPR3 films. Times of culturing are: 24 h (panels a); 48 h (panels b); C 72 h (panels c).



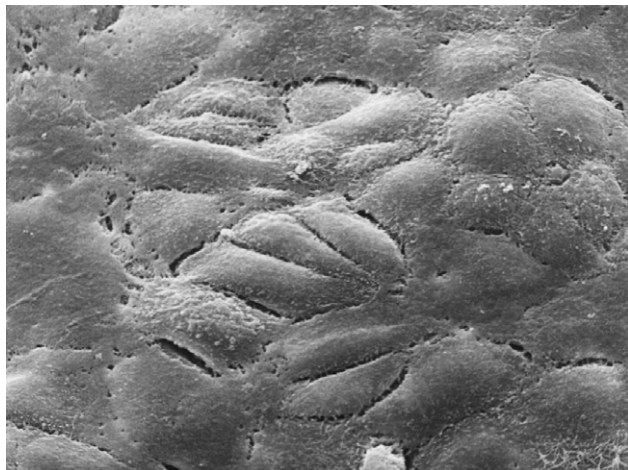


Fig. 4. Scanning electron microscopy picture of HUVEC cells after 7 days culturing on a CHPR3 film.

films seeded cells did not grow and/or start to detach from the substrate as shown also in Fig. 2.

#### 4. Conclusions

The results reported in this preliminary study show that the presence of sucrose or raffinose at a high concentration along with phosphate salts in the chitosan film-forming solution affords a smooth, amorphous and highly hydrophilic material in form of soft and elastic film with optimal cytocompatibility.

Spectroscopic analysis suggested the absence of sugar in the final structure of the film. Therefore, the role of the sugar in improving cytocompatibility remains to be clarified: an increase of the viscosity of the solution during the gel formation might be claimed as one of the most probable causes responsible for the differences observed in the physicochemical and biological characteristics of the prepared films.

The films prepared from the sugar containing solutions afforded better biocompatibility owing to the higher wettability, hydrophilicity and smoother surface. It is worth to note that both human WI38 and HUVEC cells attached and grew on these novel chitosan films more efficiently than on standard chitosan films. These cells expressed the spindle-like shape (WI-38) or the cobblestone-like shape (HUVEC) indicating their ability to maintain the original histotype morphology. These characterizing aspects suggest that both cell types also maintain the proper differentiation pattern.

Considering the improved physicochemical, mechanical properties and affinity for differentiated human cells, these novel chitosan films appear as promising candidate biomaterials for tissue regeneration and repair.

The major advantages of this approach are the simplicity, low cost, improved mechanical properties and cell affinity.

Overall, we have shown the possibility to improve the biocompatibility of chitosan films by simply modifying their solid-state characteristics without having recourse to chemical reactions implying formations of covalent bonds.

#### Acknowledgement

The authors would like to thank the Italian Ministry of Education and Research (MIUR) for financial support through FIL grants.

#### References

- [1] R. Langer, J.P. Vacanti, Tissue engineering, *Science* 260 (5110) (1993) 920–926.
- [2] S.J. Shieh, J.P. Vacanti, State-of-the-art tissue engineering: from tissue engineering to organ building, *Surgery* 137 (1) (2005) 1–7.
- [3] United Network for Organ Sharing (UNOS), 2006.
- [4] R.M. Nerem, Cellular engineering, *Ann. Biomed. Eng.* 19 (5) (1991) 529–545.
- [5] T. Freier, H.S. Koh, K. Kazazian, M.S. Shoichet, Controlling cell adhesion and degradation of chitosan films by N-acetylation, *Biomaterials* 26 (29) (2005) 5872–5878.
- [6] F. Shahidi, R. Abuzaytoon, Chitin, chitosan, and co-products: chemistry, production, applications, and health effects, *Adv. Food Nutr. Res.* 49 (2005) 93–135.
- [7] D. Ren, H. Yi, W. Wang, X. Ma, The enzymatic degradation and swelling properties of chitosan matrices with different degrees of N-acetylation, *Carbohydr. Res.* 340 (15) (2005) 2403–2410.
- [8] Y. Wan, A. Yu, H. Wu, Z. Wang, D. Wen, Porous-conductive chitosan scaffolds for tissue engineering II. in vitro and in vivo degradation, *J. Mater. Sci. Mater. Med.* 16 (11) (2005) 1017–1028.
- [9] Y. Huang, S. Onyeri, M. Siewe, A. Moshfeghian, S.V. Madhally, In vitro characterization of chitosan–gelatin scaffolds for tissue engineering, *Biomaterials* 26 (36) (2005) 7616–7627.
- [10] S.B. Rao, C.P. Sharma, Use of chitosan as a biomaterial: studies on its safety and hemostatic potential, *J. Biomed. Mater. Res.* 34 (1) (1997) 21–28.
- [11] S.A. Agnihotri, N.N. Mallikarjuna, T.M. Aminabhavi, Recent advances on chitosan-based micro- and nanoparticles in drug delivery, *J. Control. Release* 100 (1) (2004) 5–28.
- [12] E. Khor, L.Y. Lim, Implantable applications of chitin and chitosan, *Biomaterials* 24 (13) (2003) 2339–2349.
- [13] O. Felt, P. Buri, R. Gurny, Chitosan: a unique polysaccharide for drug delivery, *Drug Dev. Ind. Pharm.* 24 (11) (1998) 979–993.
- [14] M.N. Kumar, A review of chitin and chitosan applications, *React. Funct. Polym.* 46 (2000) 1–27.
- [15] A. Fini, I. Orienti, The Role of Chitosan in Drug Delivery: Current and Potential Applications, *Am. J. Drug Deliv.* 1 (2003) 43–59.
- [16] C. Shi, Y. Zhu, X. Ran, M. Wang, Y. Su, T. Cheng, Therapeutic potential of chitosan and its derivatives in regenerative medicine, *J. Surg. Res.* 133 (2) (2006) 185–192.
- [17] M.A. Bonelli, R.R. Alfieri, P.G. Petronini, M. Brigotti, C. Campanini, A.F. Borghetti, Attenuated expression of 70-kDa heat shock protein in WI-38 human fibroblasts during aging in vitro, *Exp. Cell Res.* 252 (1) (1999) 20–32.
- [18] A. Pawlak, M. Mucha, Thermogravimetric and FTIR studies of chitosan blends, *Thermochim. Acta* 396 (2003) 153–166.
- [19] W.-T. Cheng, S.-Y. Lin, Processes of dehydration and rehydration of raffinose pentahydrate investigated by thermal analysis and FT-IR/DSC microscopic system, *Carbohydr. Polym.* 64 (2006) 212–217.

- [20] D.E. Bugay, W.P. Findlay, *Pharmaceutical Excipients, Characterisation by IR, Raman and NMR Spectroscopy*, Marcell Dekker Inc., New York, 1999.
- [21] K. Cai, A. Rechtenbach, J. Hao, J. Bossert, K.D. Jandt, Polysaccharide–protein surface modification of titanium via a layer-by-layer technique: characterization and cell behaviour aspects, *Biomaterials* 26 (30) (2005) 5960–5971.
- [22] J.D. Bumgardner, R. Wiser, S.H. Elder, R. Jouett, Y. Yang, J.L. Ong, Contact angle, protein adsorption and osteoblast precursor cell attachment to chitosan coatings bonded to titanium, *J. Biomater. Sci. Polym.* 14 (2003) 1401–1409.
- [23] L. Richert, P. Lavalle, E. Payan, X.Z. Shu, G.D. Prestwich, J.F. Stoltz, P. Schaaf, J.C. Voegel, C. Picart, Layer by layer buildup of polysaccharide films: physical chemistry and cellular adhesion aspects, *Langmuir* 20 (2) (2004) 448–458.
- [24] A. Martin, *Physical Pharmacy*, fourth ed., Lea & Febinger, Philadelphia, 1993.